Combination of ShuangDan Capsule and Sorafenib Inhibits Tumor Growth and Angiogenesis in Hepatocellular Carcinoma Via PI3K/Akt/mTORC1 Pathway

Wenbo Ding, PhD[1]*, Xiuwei Chen, PhD[2]*, Licheng Yang, Master[3]*,
Yaping Chen, PhD[3], Jie Song, PhD[1], Weiquan Bu, PhD[1],
Bin Feng, PhD[1], Meng Zhang, Master[3], Yi Luo, PhD[1], Xiaobin Jia, PhD[3],
and Liang Feng, PhD[3] (iD)

Abstract

Hepatocellular carcinoma (HCC) is a high mortality liver cancer. The existing treatments (transplantation, chemotherapy, and individualized treatment) with limitations. However, drug combination provides a viable option for hepatocellular carcinoma treatment. A Chinese patent medicine, ShuangDan Capsules (SDC), has been clinically prescribed to hepatocellular carcinoma patients as adjuvant therapy and has shown good antitumor activity. The purpose of this study was to investigate whether SDC could improve the anti-cancer effect and mitigate adverse reactions of sorafenib on HCC in vivo. Magnetic resonance imaging (MRI), immunohistochemistry, and western blot were executed to reveal the potential mechanisms of the combination of SDC and sorafenib on HCC. Tumors appeared hyperintense on T2 sequence images relative to the adjacent normal liver in MRI. Combination of SDC and sorafenib inhibited the progression of DEN (Diethylnitrosamine)-induced HCC. In the HepG2 xenografts model, sorafenib plus SDC exhibited greater suppression on tumor growth than individual treatment accompanied with decreased expression of VEGF, VEGFA, Ki67, CD31 and increased expression of caspase-3. Furthermore, PI3K/Akt/mTORC1 pathway was inhibited by co-administration. Sorafenib monotherapy elicited hepatotoxicity for specific expression in the up-regulated level of aspartate transaminase (AST) and AST/glutamic-pyruvic transaminase (ALT) ratio, but the co-administration could remedy this adverse effect. These dates indicated that the combination of SDC and sorafenib might offer a potential therapy for HCC.

Keywords

hepatocellular carcinoma, ShuangDan Capsule, angiogenesis, VEGFA, PI3K

Introduction

Hepatocellular carcinoma (HCC) is the most common primary malignant liver cancer, and the second leading cause of cancer-related mortality worldwide.[1,2] Current standard curative options for early HCC include liver transplantation, surgical resection, and local radiofrequency ablation. However, most of these patients suffer post-operational recurrence and metastasis.[3] For advanced unresectable HCC, systemic chemotherapy and transcatheter arterial chemoembolization are suggested but generate limited benefits.[4] Therefore, searching for novel therapeutic strategies for HCC is urgent.

Since HCC is a very vascularized tumor, the characteristics of tumor vascular disorder, irregular branching, broken basement membrane, and excessive leakage allow tumor

[1]Nanjing University of Chinese Medicine, Nanjing, P.R. China
[2]Yuhuatai District Maternity and Child Care Clinic, Nanjing, P.R. China
[3]China Pharmaceutical University, Nanjing, P.R. China

*These authors contributed equally to this work.

Corresponding Authors:
Liang Feng, China Pharmaceutical University, #639 Longmian Avenue, Jiangning District, Nanjing, 211198, P.R.China.
Email: wenmoxiushi@163.com

Xiaobin Jia, China Pharmaceutical University, #639 Longmian Avenue, Jiangning District, Nanjing, 211198, P.R.China.
Email: jiaxiaobin2015@163.com

Yi Luo, Affiliated Hospital of Integrated Traditional Chinese and Western Medicine, Nanjing University of Chinese Medicine, Nanjing, 210028, P.R. China.
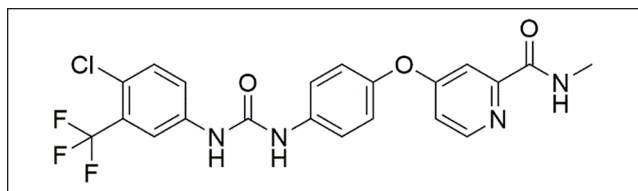Email: robertluoyi@126.com

Figure 1. Sorafenib ($C_{23}H_{28}O_{11}$).

cells to metastasize, primarily through activation of VEGF/VEGFR signaling. Therefore, inhibiting tumor angiogenesis is a crucial target of cancer treatment management.[5] PI3K mediated-pathways represent a crucial inducer of VEGF expression and blunting PI3K/Akt/mTORC1 emerges as the first alternative of antiangiogenic treatments.[6]

Sorafenib (Figure 1), a receptor tyrosine kinase inhibitor, has become the only systemic standard therapeutic approach for advanced HCC. Sorafenib can significantly prolong the survival of advanced-stage HCC patients.[7] Nevertheless, most patients remained develop resistance and the mechanisms of that are likely multifactorial, and tumor angiogenesis in HCC attenuated the functions of sorafenib.[8,9] In addition, sorafenib has been reported to induce side effects such as anorexia and hepatotoxicity.[10]

Accumulating evidence demonstrated that some traditional herbal medicines had obvious anti-cancer effects and that the use of multiple drugs in synergistic approach can enhance anti-cancer effects and overcome toxicity might be a novel therapeutic strategy for HCC.[11] ShuangDan capsule (SDC), a traditional Chinese patent medicine, consists of Moutan Cortex (derived from *Paeonia suffruticosa* Andrews, Dan-pi in Chinese) and Salviae Miltiorrhizae Radix et Rhizoma (derived from Lamiaceae *Salvia Miltiorrhiza* Bunge, Dan-shen in Chinese). The prescription has been used clinically for decades, it is considered to possess the efficacies of promoting blood circulation and removing blood stasis. In the previous study, we identified some active anti-cancer ingredients in SDC, such as sodium-tanshinol, protocatechualdehyde, paeoniflorin, rosmarinic acid, alkannic acid, salvianolic acid B and paeonol by HPLC analysis, and we found SDC combined with 5-fluorouracil (5-FU) inhibits tumor growth.[12] Some of these ingredients were reported to be effective in the prevention of tumor growth and angiogenesis.[13-16]

In the present study, we estimated the anti-angiogenic and the antitumor efficacy of SDC and sorafenib, alone and in combination. Expression of PI3K/Akt/ mTORC1 pathway-related proteins in tumors was inspected to reveal the underlying mechanism involved.

Materials and Methods

Materials

ShuangDan Capsule (Lot no. 1912023) was purchased from Guangzhou Laitai Pharmaceutical Co. Ltd. Sorafenib (Nexavar, Leverkusen, Germany) was purchased from Bayer Healthcare. Dimethyl sulfoxide (DMSO) (purity >98%) and diethylnitrosamine (DEN) were purchased from Sigma-Aldrich (St. Louis, MO, USA). HPLC-grade acetonitrile was purchased from Tedia Company (Fairfield, CT, USA). Ultrapure water was produced using a Millipore Milli-Q Gradient system (Milford, MA, USA). All other reagents were of analytical grade or better.

Methods

UPLC-Q-TOF-MS analysis. Powder of 1 mg from ShuangDan Capsule was sonicated for 45 minutes with methanol, and then centrifugated at 13 000 rpm for 10 minutes. An aliquot of the supernatant was filtered through 0.22 μm filter membrane. Waters Acquity UPLC system (Waters, Milford, MA, USA) was used to conduct the chromatographic separation process. A Waters Acquity UPLC HSS T3 C18 column (100×2.1 mm, 1.8 μm, Waters, Milford, MA, USA) was used as the stationary phase. The mobile phase consisted of phase A (0.1% formic acid in water, v/v) and phase B (pure acetonitrile). The flow rate of mobile phase was 0.2 mL/min, and the gradient elution program was set as follows: 0 to 5 minutes, 2% B; 5 to 7 minutes, 2% to 10% B; 7 to 18 minutes, 10% to 13% B; 18 to 27 minutes, 13% to 30% B; 27 to 28 minutes, 30% to 36% B; 28 to 31 minutes, 36% to 2% B; 31 to 35 minutes, 2% B. The injection volume was 2 μl. The temperatures of the column oven and auto-sampler were maintained at 25°C and room temperature, respectively.

Mass spectrometry was conducted at a high-resolution mass spectrometer Waters XEVO G2-XS Q-TOF equipped with a Z-Spray electrospray ionization (ESI). The capillary voltage was set to 3.0 kV (positive mode). The desolvation gas flow was set to 600 l/hour at a temperature of 300°C, and the cone gas was set to 40 l/hour. The source temperature to 100°C. nebulizing gas (N_2), collision gas (Ar); auxiliary gas (N_2). The scan range was set at *m/z* 50 to 1200. MS^E scan mode detection: low-energy channel collision voltage 6 eV, high-energy channel collision voltage 30 to 70 eV. 0.2 ng/μl of Leucine Enkephalin at a flow rate of 0.005 ml/min was used as reference material for mass calibration before and during the sample data acquisition.

UNIFI date processing. The UNIFI informatics platform (v.1.6.0, Waters) from Waters Corporation was used to integrate data acquisition, data mining, library searching and report generation. A natural product analytical workflow within UNIFI was used to analyze the chromatographic and mass spectral components of the herbal medicine extract utilizing the various in-built tools such as a traditional medicine library, synthetic adulterant library and structure elucidation tool to effectively confirm the ingredients in the herbal product.[17,18]

The MS^E data was acquired using UPLC-Q-TOF- MS. All the MS^E raw data were transferred to the UNIFI platform for processing, the component information is automatically matched with the traditional medicine library for the identification of these main chemical components. The identification parameters for the components in UNIFI were set as follows: In 3D peak detection, the background noise filter was set to high, apply lock mass correction. The target match tolerance, fragment match tolerance, and detected components tolerance were set to 20 mDa. Mass error was set for ± 3 mDa. After processing the data using the method above, we set up parameters to filter a large amount of false-positive results. The results were filtered by Mass Defect Filter, which is ± 5 mDa, and common fragment.

Rats, mice and cell lines. The 4-week-old male Sprague-Dawley (SD) rats (weighing 130 ± 15 g) were purchased from Comparative Medicine Center of Yangzhou University (License No: SCXK (Su) 2017-0007) and kept in a room on a 12 h light/dark cycle and at a temperature of 23°C to 25°C and $50\% \pm 5\%$ humidity. Four to 6-week-old BALB/c male nude mice were purchased from the Comparative Medicine Center of Yangzhou University (License No: SCXK (Su) 2017-0007) and housed in an isolator and fed with autoclaved food *ad libitum*. All experiments were approved by Affiliated Hospital of Integrated Traditional Chinese and Western Medicine, Nanjing University of Chinese Medicine.

The human hepatoma cell line HepG2 was purchased from the Cell Bank of the Chinese Academic of Sciences (Shanghai, China). The HepG2 cells were maintained at 37°C at 5% CO_2 in Dulbecco's modified Eagle's medium (DMEM) (HyClone, Logan, UT, USA) supplemented with 10% FBS (Wisent, Quebec, Canada), 100 U/ml penicillin and 100 μg/ml streptomycin (Boytime, Jiangsu, China).

Animal model and treatment. The experimental rats were injected intraperitoneally with DEN (70 mg/kg) once a week for 10 weeks. Then the rats were randomly divided into 4 groups (n=6): the control group (0.9% saline), the SDC group (33.4 mg/kg), the sorafenib group (13.4 mg/kg), and the combined group (sorafenib with 13.4 mg/kg plus SDC with 33.4 mg/kg). From week 11 to 20, each group received daily treatment (intragastric administration), and the volume of the intragastric drug instillation was 1 mL/kg. Rats were sacrificed by cervical vertebrae dislocation after the last administration. The doses of SDC were selected based on our previous studies.

HepG2 cells were subcutaneously injected into the dorsal region of each mouse. Tumors were measured at the start of treatment by vernier calipers every 3 days. Tumor volume was calculated using the formula (length $\times$ width^2)/2.[19] Mice were randomized to 4 groups and then treated with 0.9% normal saline, SDC (50 mg/kg) and/or Sorafenib (20 mg/kg) by daily gavage for 4 weeks (n=4). After 4 weeks, mice were sacrificed.

Magnetic resonance imaging (MRI). MRI was performed once a week since week 8 to monitor tumor formation. Rats were anesthetized by a gas anesthesia machine (Matrix VMP; GENE&I, Beijing, China) with 2% isoflurane in the mixture of 20% oxygen/80% room air, and then were placed in specific wrist coil (Chenguang Medical Technologies Co., Ltd, Shanghai, China). A supine position was scanned for imaging acquisition using a 1.5 T MRI scanner (Echo speed; GE, Milwaukee, WI). DWI, T1 SPGR, and T2 FRF SE sequences were executed.

In vivo tumorigenesis assay. The tumors of mice were subjected to histological examination, and the excised tissues were fixed for hematoxylin and eosin (H&E) staining.

Immunohistochemistry. The immunohistochemical staining was performed according to previous description.[20] Heat-induced epitope retrieval was achieved with Tris–EDTA (pH 8) at 98°C for 40 minutes. Endogenous peroxidase activity was quenched by treatment with 3% H_2O_2 for 10 minutes. Sections (4 μm thick) from paraformaldehyde-fixed HepG2 tumors were stained with rabbit anti-human polyclonal Ki67, caspase 3 and rabbit anti-human monoclonal VEGFA, CD31 antibodies (1: 1000, Abcam, Cambridge, MA), followed by incubation with horseradish peroxidase-conjugated secondary antibody. Sections were then incubated with developing solution, and counterstained with hematoxylin. Color was fixed with acid alcohol and dehydration steps. The number of microvessels per field was scored by averaging 5 field counts for each group.

In vivo matrigel plug angiogenesis assay of mice. Angiogenesis in vivo was verified via the Matrigel plug assay. Matrigel (0.5 ml/plug) in liquid (BD Biosciences) contained VEGF (150 ng/ml) and then drugs were added: vehicle, sorafenib (15 mg/kg), SDC (2 mg/kg), or the combination of sorafenib and SDC. Matrigel mixes were injected subcutaneously in the mid-ventral abdominal region of each mouse. Mice were sacrificed and the plugs were completely excised and photographed. Matrigel was collected, the content of hemoglobin was measured using a hemoglobin assay kit (Sigma-Aldrich, St. Louis, MO, USA), according to manufacturer's protocols.[21,22]

Western blotting. Total protein was extracted from HepG2 tumors after lysis in RIPA buffer (Sigma-Aldrich, St Louis, MO, USA). The protein concentrations of the supernatants were determined by the BCA protein assay kit. Equal amounts of protein (50 μg) were separated by 12% SDS-PAGE and transferred onto PVDF membranes.

The membranes were incubated with primary antibodies (anti-p-PI3K, anti-p-Akt, anti-Akt, anti-mTORC1 anti-p-mTORC1, anti-PI3K, and anti-GAPDH) (Santa Cruz Biotechnology, USA) at 4°C overnight. After washing with TBST, the membrane was incubated with horseradish peroxidase-conjugated goat anti-rabbit immunoglobulin G secondary antibody (Shanghai Kangcheng Biological Engineering Co., Ltd., Shanghai, China) for 1 hour at room temperature. Then, the protein level was quantified by ECL Substrate (ECL; Bio-Rad Laboratories, Inc., Hercules, CA, USA) and image acquisition was analyzed in Chemi-Doc XRS system (BIO-RAD, USA).

ELISA for VEGF, ALT, and AST levels. VEGF levels in homogenates of tumor tissues or in blood samples of HepG2 nude mice were assessed by Quantikine ELISA VEGF kit (R&D, Shanghai, China) according to the manufacturer's protocols. Alanine aminotransferase (ALT) and aspartate aminotransferase (AST) in blood samples were assessed by a Biochemical Automatic Analyzer Hitachi 7080 (Hitachi, Ltd, Tokyo, Japan).

Statistical analysis. The GraphPad Prism 5.0 software (Graph Pad Software Inc., San Diego, CA, USA) was used for the statistical analysis. Statistical comparisons were performed using one-way ANOVA followed by Tukey's multiple comparison post hoc tests and $P < .05$ were considered considerably different. The results were presented as the means ± SD.

Results

UPLC-Q-TOF-MS Analysis Chemical Components of SDC

The compounds of SDC extract were detected by UPLC-Q-TOF-MS (the base peak chromatograms of SDC in positive ion modes was shown in Figure 2) then the data acquired by MS^E were analyzed using UNIFI software. Following the UNIFI-mediated data processing, 30 compounds (Table S1) were rapidly detected and identified. The data processing method was described in Section 1.2.2. Table S1 shows the summary plot of the identified components. Each listed chemical component contains the following information: compound name, formula, retention time, exact mass error in ppm, ionization mode, adduct ions, and fragments ions *m/z*. Compounds with good matches can be confirmed.

Combination of SDC With Sorafenib on the Progression of DEN-Induced HCC

Therapeutic efficacy of sorafenib plus SDC was examined by comparing tumor size from MRI images, physical examination of the excised liver, as well as histological staining at end-point necropsy. The liver tumors appeared homogeneously hypo- or isointense on T1 weighted MRI images relative to the adjacent normal liver, as indicated with asterisk in Figure 3 (the upper panel). Combination group revealed an obvious inhibition on tumor nodules than DEN group as manifested in MRI analysis.

The histologic analysis also confirmed the development of HCC after DEN treatment. Tumor cells, necrosis, and hemorrhage were observed in DEN group. Moreover, dilation of hepatic sinus and infiltration of inflammatory cells were surrounded by tumors in DEN group. In both SDC group and sorafenib group, tumor formation was attenuated compared with DEN group, but fibrosis and inflammatory cell infiltration were still obvious (Figure 3, the lower panel). The combination of SDC and sorafenib markedly reduced the number of cancerous cells as shown in H&E staining, confirming that the co-treatment is superior to the single treatment.

Combination of SDC With Sorafenib on the Growth of HepG2 Tumors

SDC or sorafenib alone exhibited an insignificant effect against HepG2 xenograft tumors (Figure 4A). Although the average tumor volume treated with SDC or sorafenib was smaller than the control group, there were no statistical differences. The combination of SDC with sorafenib elicited an extremely strong tumor regression. Within 26 days of co-treatment, tumor volume was abridged by half (to $540 \pm 110 \, mm^3$) and by 32 days of co-treatment tumors were barely palpable. In summary, these results indicate that sorafenib and SDC were able to encourage substantial regression of established xenografts (Figure 4B).

Sorafenib has been reported to induce hepatotoxicity. Clinically, the secretion of ALT and AST of HCC patients are routinely examined to avoid potential hepatotoxicity. ALT and AST levels in the plasma of HepG2 xenograft mice were examined at the endpoint of the experiment. The level of AST as well as the AST/ALT ratio was augmented after sorafenib monotherapy ($P < .05$, Figure 4C). The combination could attenuate the secretion of AST stimulated by sorafenib ($P < .05$).

Combined Treatment on Cell Proliferation and Apoptosis Markers in HepG2 Tumors

The proliferation biomarker Ki-67 was considerably reduced in sorafenib group ($P < .05$ vs control). Ki-67 was significantly abridged by combined therapy of sorafenib and SDC ($P < .01$ vs control, Figure 5, the upper panel). Thus, the combined treatment was superior to alone treatment in constraining cell proliferation of HepG2 xenograft tumors. Moreover, the apoptosis marker caspase 3 was
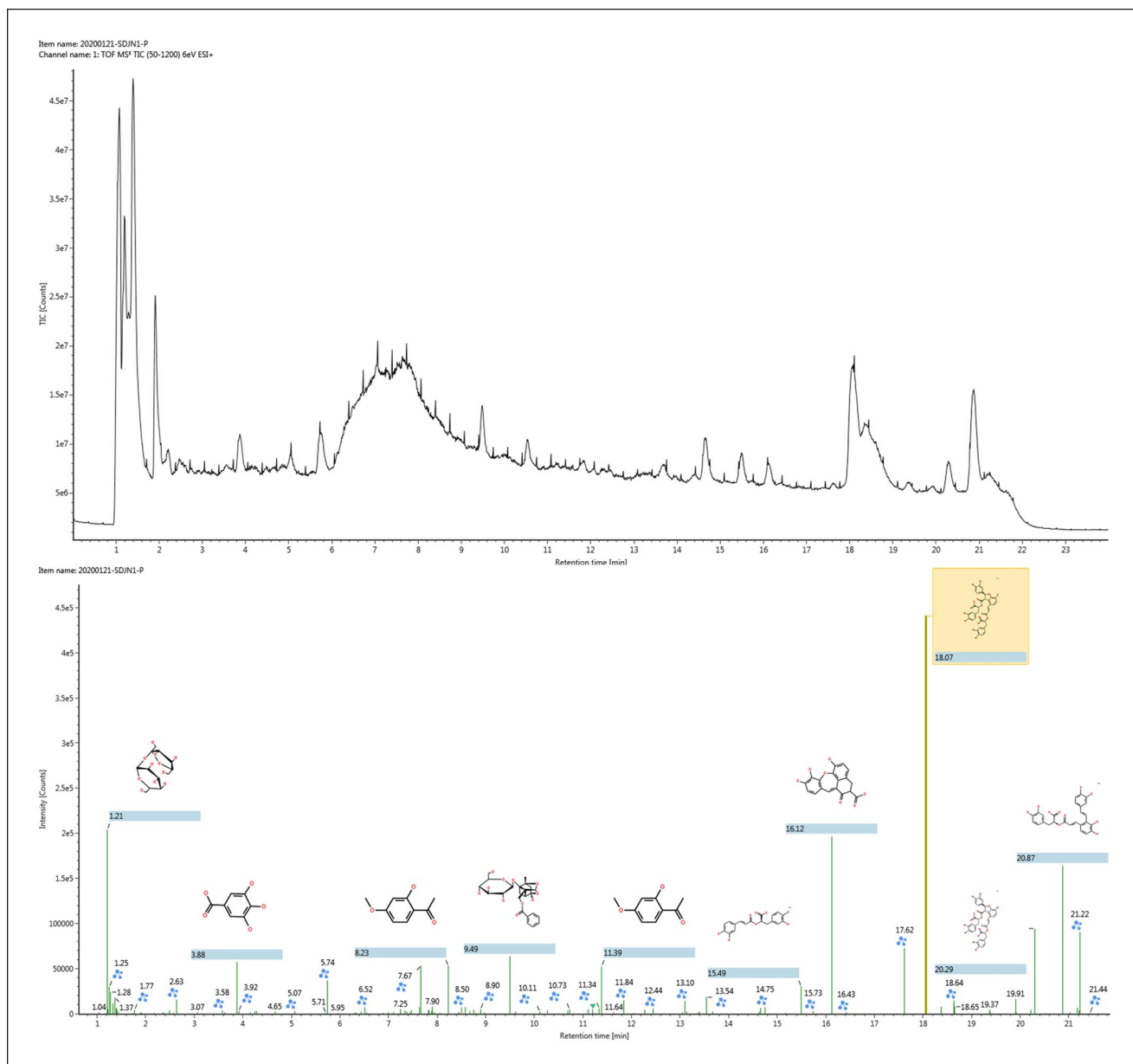
Figure 2. The base peak chromatogram of SDC extract by UPLC-Q-TOF-MS (upper panel) and the sketch map of automated structural identification of components in SDC by UNIFI (lower panel). The signals were automatically identified according to MS^E data matching.

remarkably up-regulated in combination group than either sorafenib or SDC alone (Figure 5, the lower panel).

IHC Analysis of the Effects of Co-treatment on Blood Flow and Vascularity in HepG2 Tumors Bearing-Nude Mice

It is worth mentioning that throughout gross examination of the resected tumors, there was less blood vessels on the surface of the tumors that exposed to combination treatment

(Figure 4A). To confirm whether this was caused by inhibition on vasculature, the angiogenesis marker CD31 was identified by immunohistochemistry to reflect microvessel density (MVD). CD31-positive blood vessels in tumors treated by the combination of sorafenib and SDC were significantly decreased ($P<.01$, vs the control group). The control group had the highest MVD, followed by SDC, then sorafenib, and then the combination (Figure 6A). H&E assays of the tumor sections were further executed to reveal the effect of treatment on vascularity. Consistent with the
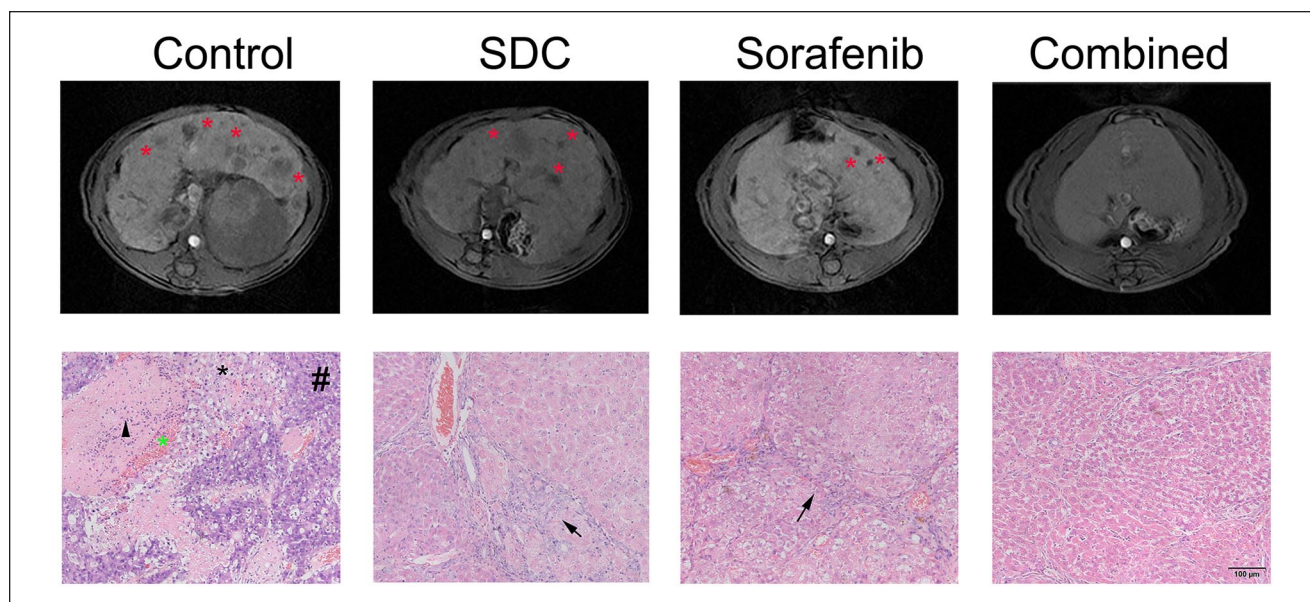
Figure 3. The combination of SDC and Sorafenib inhibited HCC development after DEN insult. The upper panel is representative T2-weighted MRI images of rat liver in the axial positions at week 28. Tumor nodules in MRI were indicated with red asterisk. The lower panel is representative H&E-stained liver sections. Hemorrhage (leftward asterisk), hepatic sinus dilation and inflammatory cells infiltration (black arrow head), tumor cells (hash symbol) and necrosis (rightward asterisk) were obvious in DEN group. Black arrow means fibrosis.

results from immunohistochemistry staining, the least amount of blood vessels was observed in the combination group as shown in H&E assays (Figure 6B). In vivo Matrigel plug angiogenesis analyses were performed to examine the effects of combined treatment on hemoglobin contents. Matrigels containing the combination drugs yielded the least hemoglobin contents than Matrigels from vehicle, sorafenib, or SDC group (Figure 6C).

Co-treatment on the Plasma and Tumor Tissue Level of VEGF

VEGF is the primary mediator of angiogenesis in primary tumors. In immunohistochemistry analysis, there was no significant difference in the number of VEGFA positive cells between SDC and the control group. But the addition of SDC to sorafenib significantly decreased the intensity of VEGFA ($P < .01$, Figure 7A). We found that sorafenib plus SDC were capable of decreasing VEGF levels in tumor tissues ($P < .05$, Figure 7B); although the effect of the mono-therapy group was negligible.

To examine why the combination of SDC with sorafenib was more effective than SDC alone or sorafenib alone, we surveyed the effect on signal transduction and analyzed protein expression in tumor lysates by western blotting. SDC treatment showed limited regulation on the activation of PI3K/AKT signaling. PI3K and downstream Akt and mTORC1 phosphorylation were repressed in sorafenib plus SDC group ($P < .01$ vs the control group, Figure 8).

Discussion

Among the compounds of SDC, sodium-tanshinol and salvianolic acid B have been reported to be effective in the prevention of tumor growth and angiogenesis.[13] Moreover, paeoniflorin inhibited human gastric carcinoma cell proliferation partly through the suppression of PI3K/Akt signaling.[14] Sodium-tanshinol, the major water-soluble component of Salviae Miltiorrhizae Radix et Rhizoma, had the anti-tumor activity in B16F10 melanoma by inhibiting angiogenesis and tumor cell invasion.[15] Paeonol oxime inhibited bFGF-induced angiogenesis and reduced VEGF levels in fibrosarcoma cells.[16] In a previous study, we found SDC combined with 5-FU inhibits tumor angiogenesis by inhibiting VEGF and MMP2 expression, thereby blocking tumor growth in the human liver cancer cell line Huh-7 and tumor bearing mice, and the effects are better than single administration group.[12]

Currently, several HCC animal models have been established. DEN-induced HCC model in rodents can resemble human HCCs in terms of disease progression and histopathological features with diverse differentiation and vascularity. This model has been successfully applied to predict the diagnostic potentials of specific MRI contrast agents after inducing 8 to 10 weeks.[23-26] Xenograft models of HCC allow for reproducible tumors that are spotted with short latencies, but lack the tumor microenvironment which characterizes human pathogenesis.[27] Likewise, the orthotopic tumor model fails to mimic the phenotypic background of cirrhosis. The DEN-induced rat HCC model displayed
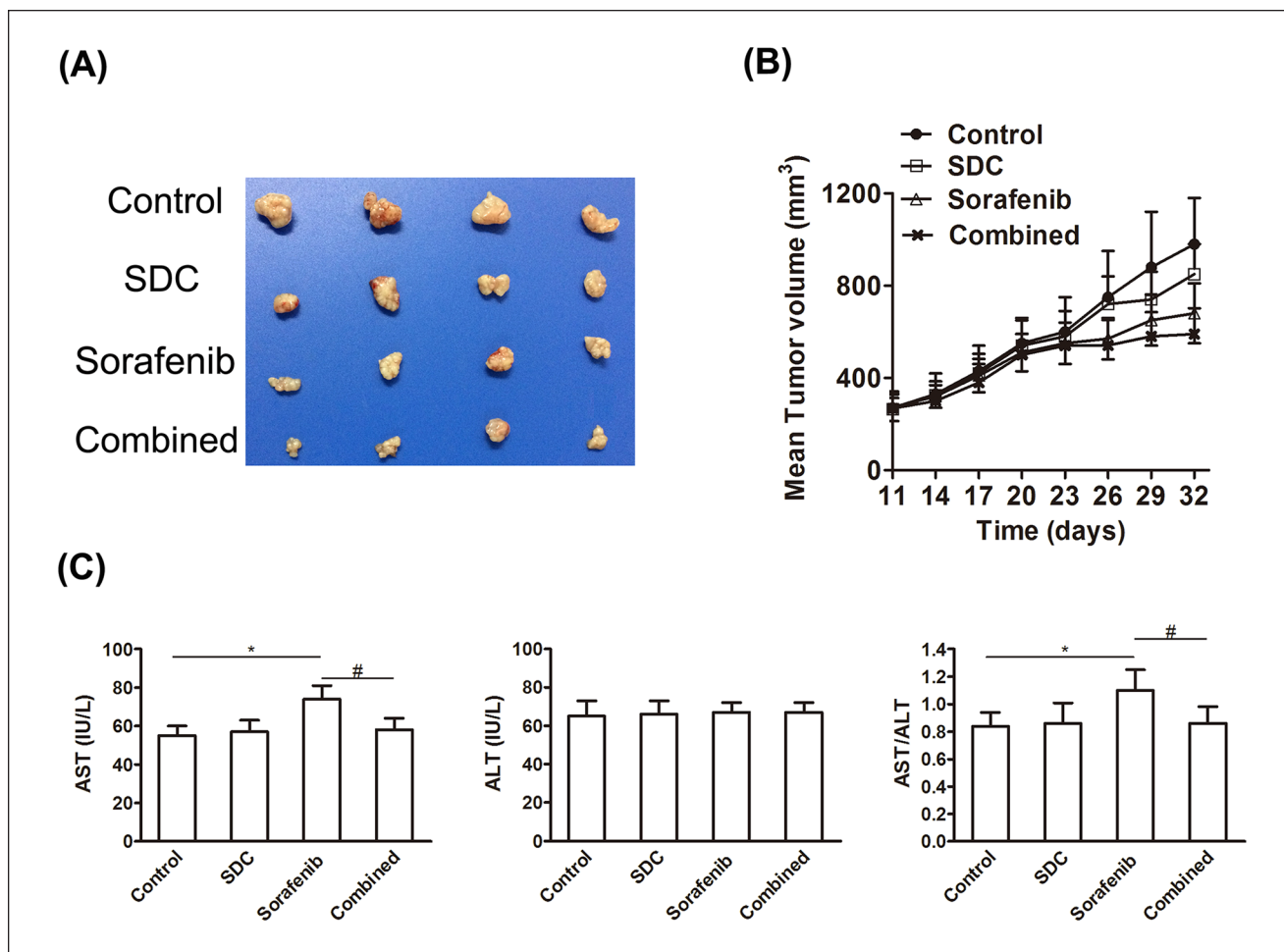
Figure 4. SDC enhanced the antitumor efficacy of Sorafenib in nude mice. (A) Tumor size. Representative pictures of tumors from each group. The picture was taken on the 32nd day after implantation. Mice were treated with saline; Sorafenib alone at 20 mg/kg; SDC alone at 50 mg/kg; Sorafenib 20 mg/kg plus SDC 50 mg/kg (SDC was given 1 hour before Sorafenib administration). (B) Changes in tumor volume in 32 days. Each point represents the mean ± SD of tumor volumes from 4 mice in each group. (C) SDC attenuated hepatotoxicity induced by Sorafenib. Serum levels of AST, ALT, and the ratio of AST/ALT in SDC group, Sorafenib group, and the combination, #$P < .05$, compared with the control group, *$P < .05$, compared with sorafenib group.

multifocal HCC in a chronically damaged liver background, with the advantage of producing phenotypic changes reflective of human disease and reproducibility. DEN tumors showed lower mean growth rates and 18F-fluorodeoxyglucose uptake and higher perfusion and diffusion values than orthotopically implanted HCC tumors.[25] In the present study, we used nude-mouse HepG2 xenografts model and DEN-induced HCC model to estimate the anti-angiogenic and the antitumor efficacy of SDC and sorafenib, alone and in combination. The expression of angiogenesis-related proteins in tumors was inspected to reveal the underlying mechanism. Human HCC is a major health problem worldwide. The lack of effective chemotherapy significantly contributes to high mortality. Drug combinations have been widely used in treating cancer for the synergistic effect. This study revealed that SDC efficaciously increased the

inhibitory effect of sorafenib on HCC tumor growth, as well as reducing angiogenesis in nude mice. SDC plus sorafenib also inhibited the proliferation marker Ki67 and promoted the expression of the apoptosis marker caspase-3. Hepatocellular regeneration and bile duct hyperplasia have also been observed in DEN-induced liver in this study. Therefore, both xenograft model and DEN model of HCC were used to reflect the synergistic effect of the combination of SDC and sorafenib.

Activation of the AKT/mTOR cascade is one of the most frequent events along hepatocarcinogenesis. Abnormal activation of the PI3K/Akt/mTOR pathway has been found in HCC.[28] Akt induces mTORC1, which in turn involves the translation of VEGF. In human HCC, Akt activation has been reported in 50% of tumor specimens, and is related with aggressive tumor growth and poor prognosis.[29] Tumor
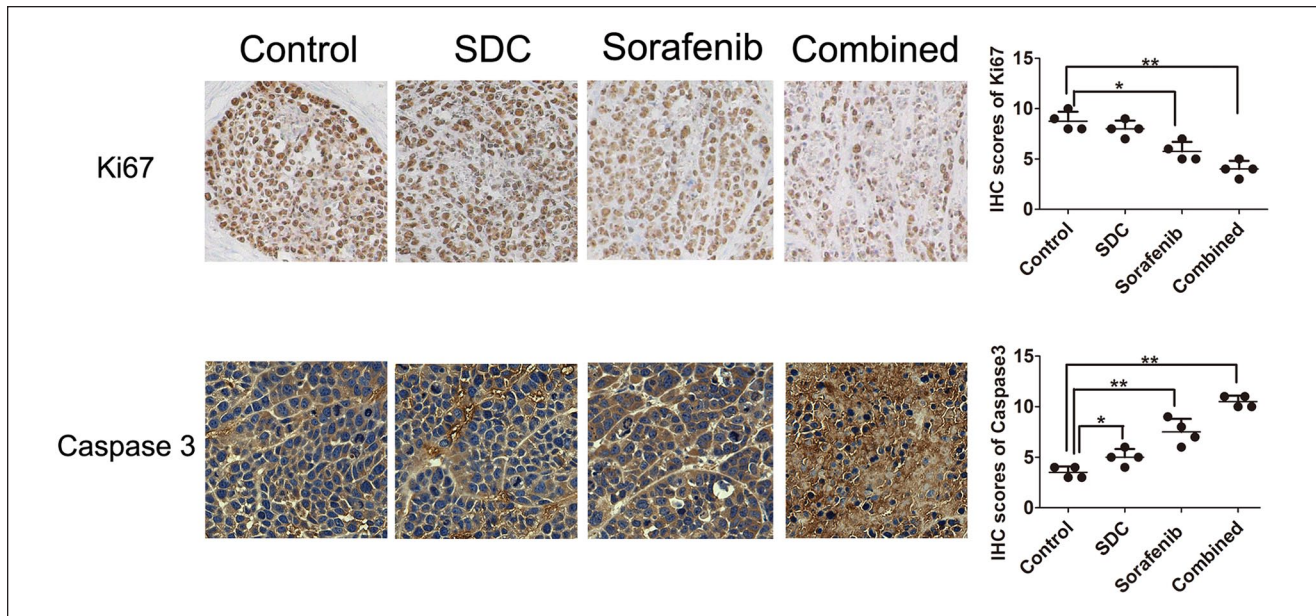
Figure 5. Effects of sorafenib combined with SDC on the expression of Ki67 and caspase 3 and the IHC scores for each group. The intensities of Ki-67 were decreased after combined therapy compared with the sorafenib or SDC mono-therapy using immunohistochemical (IHC), while caspase 3 was increased in the combination therapy. Magnification, ×100. *$P < .05$, **$P < .01$ versus the control group.

angiogenesis is required for HCC development, enabling the distinction of dysplastic and tumor nodules.[30] Pro-angiogenic factors secreted by tumors yield an abnormal vascular network characterized by permeable, immature and disorganized blood vessels, leading to poorly perfused tumors.[31] Due to CD31′s endothelial cell specificity, it is the most common marker to detect angiogenesis and is widely used to detect the presence of microvasculature. MVD is used to quantitatively define the degree of neovascularization and angiogenesis.[32,33] Amplified MVD is considered as a noteworthy and independent prognostic indicator in human cancers.[34-36] In the gross examination of the resected HepG2 tumors, the least number of blood vessels was observed in the combination group among all the groups. Moreover, both H&E staining and immunohistochemistry assays verified that sorafenib combined with SDC decreased angiogenesis.

VEGF plays a significant role in angiogenesis and serves as a validated target for cancer therapy.[37,38] VEGF level is motivated by oncogenes including ERBB2, Src, Ras, and so on.[39] As the most specific and potent proangiogenic factor, VEGFA is important in the metastasis and tumor growth of liver cancer, head and neck tumors, cervical cancer, renal cell cancer, as well as breast cancer and colorectal cancer.[40] High expression of VEGFA was associated with high MVD in most reported studies.[41] Endothelial cell proliferation, differentiation, and migration are triggered when VEGFA binds to its receptors and activates manifold signal cascades. VEGFA intermediates and promotes vascular permeability,

thus increasing tumor dissemination via circulation. By regulating tumor growth and metastasis through PI3K/AKT and MAPK/ERK1/ERK2 pathway, VEGFA protects new vasculature against destruction.[42] In immunohistochemistry tests, the combination of sorafenib and SDC reduced VEGFA positive cells, as well as decreased VEGF levels in tumor tissues.

Actually, there have been clinical case reports indicating that sorafenib can cause lethal hepatotoxicity.[43] In this study, sorafenib augmented the AST level in mice bearing HepG2 xenograft, signifying potential hepatotoxicity. However, SDC does not produce obvious adverse effects during treated animals. Nude mice in the SDC treatment remained equally active and the combination mitigated the increment of AST levels. Of note, sorafenib-induced hepatotoxicity causes hepatocyte injury, which may further cause the release of inflammatory factors, thus promoting tumor growth. Inflammation does exert pleiotropic effects in the development of cancer, such as malignant transformation, resistance to growth inhibition, escape of programmed cell death, enhanced angiogenesis, tumor growth, invasion, and metastatic spread.[44,45] Coincidentally, some ingredients of SDC demonstrated positive effects on different inflammatory diseases, models of liver injury and human HCC cell lines. Tanshinol is widely concerned about its anti-inflammatory properties in various diseases, and salvianolic acid B suppresses the proinflammatory activity by inhibiting JNK.[46,47] Paeoniflorin treatment has shown protective and anti-inflammatory effects against several
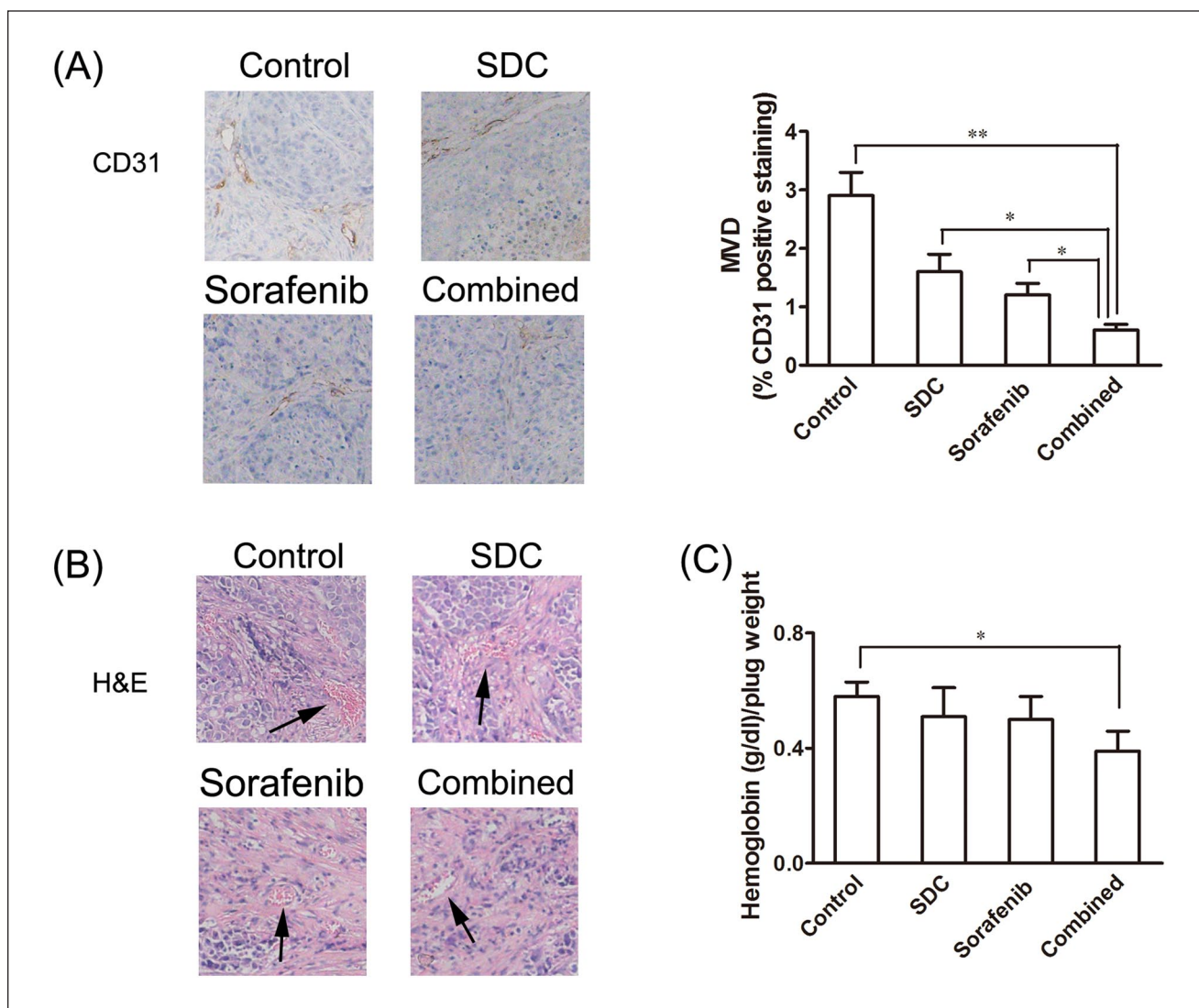
Figure 6. Sorafenib-SDC combined treatment led to a significant decrease in tumor vascularity in xenograft mice. (A) Expression of CD31. Tumor tissues in each group were resected and immune-stained with anti-CD31 antibodies (using DAB). MVD was quantified in tumor samples stained with CD31. The combination group showed the lowest MVD (0.6%) compared to control (2.9%), sorafenib alone (1.2%), and SDC alone (1.6%) treated groups. (B) H&E staining of tumors demonstrated the least amount of vasculature in the combination group. (C) In vivo angiogenesis was performed by Matrigel plug assay. The Matrigel plug with combined drugs had the lowest hemoglobin contents (0.39) compared to Matrigel plug with control (0.58), sorafenib alone (0.50), and SDC alone (0.51). *P<.05, **P<.01 versus the control group.

liver diseases by inhibiting multiple signal pathways and blocking the release of inflammatory factors, and also induced apoptosis in hepatocellular carcinoma cells.[48-51] Paeonol can alleviate various liver injuries via inhibiting inflammation and inhibit the proliferation of a variety of human HCC cells and downregulates the oncogene AKT in the cell lines.[52-54] CD31 promotes hepatic inflammatory in APAP-induced inflammatory, and the rise in circulating soluble (s)CD31 during inflammatory diseases[55,56] Danshen extract ameliorates DSS-induced ulcerative colitis in mice associated with inhibition of TLR4/PI3K/AKT/mTOR signaling pathway.[57] According to our previous and current studies, SDC reduces CD31 and suppresses the PI3K/AKT/mTOR pathway.

Future studies are warranted to ensure whether the synergic effect is owing to the fact that SDC could mitigate the hepatocyte injury and improve the inflammatory environment, and to clarify exactly which inflammatory-induced tumor growth pathways are improved by SDC.

Conclusions

The major finding of this study is that SDC synergistically increases the anticancer efficacy of sorafenib through
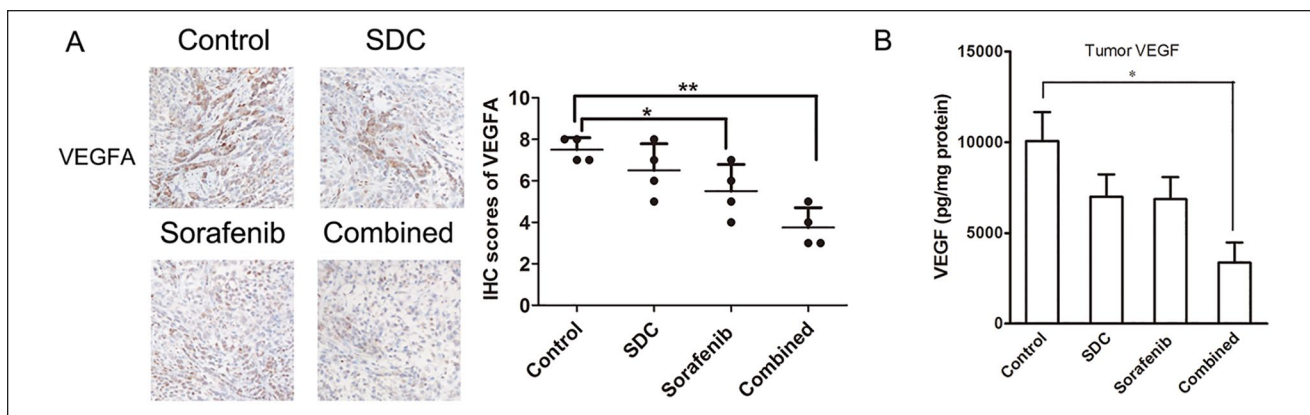
Figure 7. Effects of sorafenib combined with SDC on the expression of VEGFA and the level VEGF. (A) Expression of VEGFA and the IHC scores for each group. Tumor tissues in each group were resected and immune-stained with anti-VEGFA antibodies by IHC assays. Magnification, ×100. (B) Levels of VEGF protein expression in tumors. Tumor samples were collected on day 32 (n = 4). *$P < .05$, **$P < .01$ versus the control group.
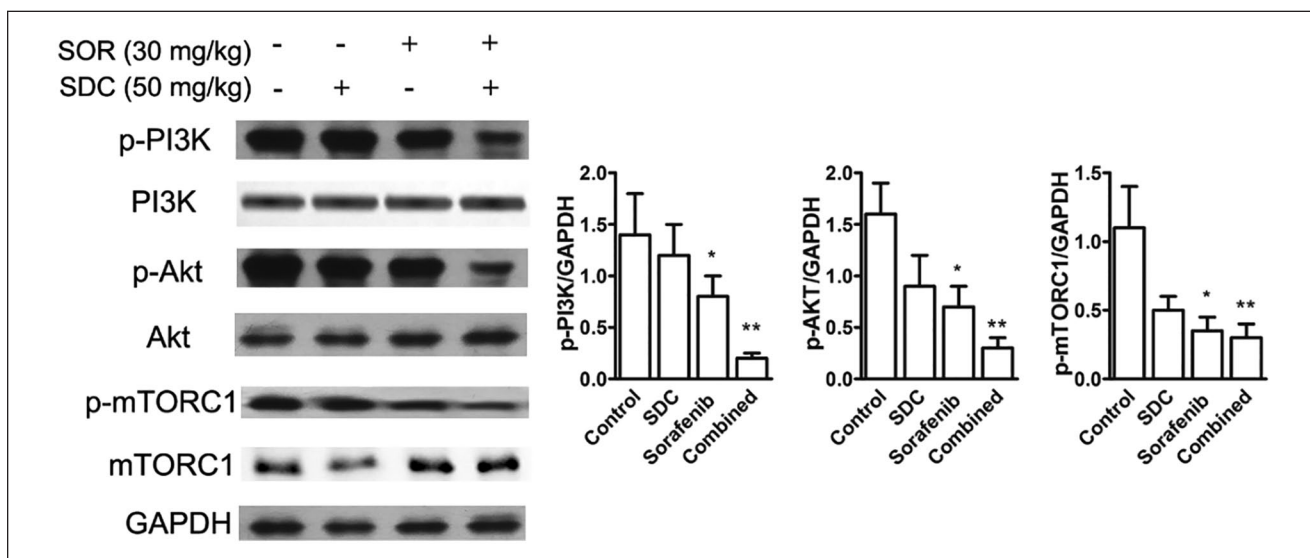

Figure 8. Combined treatment of SDC plus sorafenib affected PI3K/Akt pathways. Tumor lysates were collected and subjected to western blotting by using antibodies to p-PI3K, PI3K, p-Akt, Akt, p-mTORC1, and mTORC1 and relative expression levels analyzed by Image J software (right) were shown. Bars represent the mean ± SD. *$P < .05$, **$P < .01$ versus the control group.

suppression of angiogenesis and the PI3K/Akt/mTORC1 pathway in vivo, and remedies an adverse effect (hepatotoxicity). These results suggest that the combination of SDC and sorafenib may be a potential therapeutic for patients with advanced HCC.

Availability of Data and Materials

All data are available from the corresponding author on reasonable request.

Declaration of Conflicting Interests

The author(s) declared no potential conflicts of interest with respect to the research, authorship, and/or publication of this article.

Ethics Approval and Consent to Participate

All animal experiments were approved by Affiliated Hospital of Integrated Traditional Chinese and Western Medicine, Nanjing University of Chinese Medicine under the approval number AEWC-20170726-21.

ORCID iD

Liang Feng ⓘD https://orcid.org/0000-0003-4807-7480

Supplemental Material

Supplemental material for this article is available online.

References

1. Dhanasekaran R, Venkatesh SK, Torbenson MS, Roberts LR. Clinical implications of basic research in hepatocellular carcinoma. *J Hepatol*. 2016;64:736-745.

2. Ferlay J, Soerjomataram I, Dikshit R, et al. Cancer incidence and mortality worldwide: sources, methods and major patterns in GLOBOCAN 2012. *Int J Cancer*. 2015;136:E359-E386.

3. Ruan J, Zheng H, Rong X, et al. Over-expression of cathepsin B in hepatocellular carcinomas predicts poor prognosis of HCC patients. *Mol Cancer*. 2016;15:17.

4. Yu X, Tang W, Yang Y, et al. Long noncoding RNA NKILA enhances the anti-cancer effects of baicalein in hepatocellular carcinoma via the regulation of NF-κB signaling. *Chem Biol Interact*. 2018;285:48-58.

5. Ramjiawan RR, Griffioen AW, Duda DG. Anti-angiogenesis for cancer revisited: is there a role for combinations with immunotherapy? *Angiogenesis*. 2017;20:185-204.

6. Yang H, Wang J, Fan JH, et al. Ilexgenin a exerts anti-inflammation and anti-angiogenesis effects through inhibition of STAT3 and PI3K pathways and exhibits synergistic effects with Sorafenib on hepatoma growth. *Toxicol Appl Pharmacol*. 2017;315:90-101.

7. Llovet JM, Ricci S, Mazzaferro V, et al. Sorafenib in advanced hepatocellular carcinoma. *New Engl J Med*. 2008;359:378-390.

8. Shi S, Rao Q, Zhang C, Zhang X, Qin Y, Niu Z. Dendritic cells pulsed with exosomes in combination with PD-1 antibody increase the efficacy of sorafenib in hepatocellular carcinoma model. *Transl Oncol*. 2018;11:250-258.

9. Shen J, Jiang F, Yang Y, et al. 14-3-3η is a novel growth-promoting and angiogenic factor in hepatocellular carcinoma. *J Hepatol*. 2016;65:953-962.

10. Rudalska R, Dauch D, Longerich T, et al. In vivo RNAi screening identifies a mechanism of sorafenib resistance in liver cancer. *Nat Med*. 2014;20:1138-1146.

11. Zhang J, Hu J, Chan HF, Skibba M, Liang G, Chen M. iRGD decorated lipid-polymer hybrid nanoparticles for targeted co-delivery of doxorubicin and sorafenib to enhance anti-hepatocellular carcinoma efficacy. *Nanomedicine*. 2016;12:1303-1311.

12. Ding WB, Ning Q, Xia Z. Study on synergistic anti-tumor effect of Shuangdan Capsules combined with 5-FU on hepatocellular carcinoma cells Huh-7 and xenograft mice. *Zhongguo Zhong Yao Za Zhi*. 2020;45:5762-5769.

13. Yang Y, Zhang L, La X, Li Z, Li H, Guo S. Salvianolic acid A inhibits tumor-associated angiogenesis by blocking GRP78 secretion. *Naunyn Schmiedebergs Arch Pharmacol*. 2019;392:467-480.

14. Zheng YB, Xiao GC, Tong SL, et al. Paeoniflorin inhibits human gastric carcinoma cell proliferation through up-regulation of microRNA-124 and suppression of PI3K/Akt and STAT3 signaling. *World J Gastroenterol*. 2015;21:7197-7207.

15. Zhang LJ, Chen L, Lu Y, et al. Danshensu has anti-tumor activity in B16F10 melanoma by inhibiting angiogenesis and tumor cell invasion. *Eur J Pharmacol*. 2010;643:195-201.

16. Lee HJ, Kim SA, Lee HJ, et al. Paeonol oxime inhibits bFGF-induced angiogenesis and reduces VEGF levels in fibrosarcoma cells. *PLoS One*. 2010;5:e12358.

17. Chen K, Liu X, Wu X, Xu J, Dong F, Zheng Y. The degradation dynamics and rapid detection of thiacloprid and its degradation products in water and soil by UHPLC-QTOF-MS. *Chemosphere*. 2021;263:127960.

18. Mi N, Cheng T, Li H, et al. Metabolite profiling of traditional Chinese medicine formula Dan Zhi tablet: an integrated strategy based on UPLC-QTOF/MS combined with multivariate statistical analysis. *J Pharm Biomed Anal*. 2019;164:70-85.

19. Osborne CK, Hobbs K, Clark GM. Effect of estrogens and antiestrogens on growth of human breast cancer cells in athymic nude mice. *Cancer Res*. 1985;45:584-590.

20. Chen M, Sun R, Shi B, et al. Antitumor efficacy of chimeric antigen receptor T cells against EGFRvIII-expressing glioblastoma in C57BL/6 mice. *Biomed Pharmacother*. 2019;113:108734.

21. Lee JG, Wu R. Erlotinib-cisplatin combination inhibits growth and angiogenesis through c-MYC and HIF-1α in EGFR-mutated lung cancer in vitro and in vivo. *Neoplasia*. 2015;17:190-200.

22. Kastana P, Zahra FT, Ntenekou D, et al. Matrigel plug assay for in vivo evaluation of angiogenesis. *Methods Mol Biol*. 2019;1952:219-232.

23. Su B, Luo T, Zhu J, et al. Interleukin-1β/Iinterleukin-1 receptor-associated kinase 1 inflammatory signaling contributes to persistent Gankyrin activation during hepatocarcinogenesis. *Hepatology*. 2015;61:585-597.

24. Liu Y, De Keyzer F, Wang Y, et al. The first study on therapeutic efficacies of a vascular disrupting agent CA4P among primary hepatocellular carcinomas with a full spectrum of differentiation and vascularity: correlation of MRI-microangiography-histopathology in rats. *Int J Cancer*. 2018;143:1817-1828.

25. Groß C, Steiger K, Sayyed S, et al. Model matters: differences in orthotopic rat hepatocellular carcinoma physiology determine therapy response to sorafenib. *Clin Cancer Res*. 2015;21:4440-4450.

26. Tang Q, Wang Q, Zhang Q, et al. Gene expression, regulation of DEN and HBx induced HCC mice models and comparisons of tumor, para-tumor and normal tissues. *BMC Cancer*. 2017;17:862.

27. Kiefer RM, Hunt SJ, Pulido S, et al. Relative initial weight is associated with improved survival without altering tumor latency in a translational rat model of diethylnitrosamine-induced hepatocellular carcinoma and transarterial embolization. *J Vasc Interv Radiol*. 2017;28:1043-1050.e2.

28. Zhou Q, Lui VW, Yeo W. Targeting the PI3K/Akt/mTOR pathway in hepatocellular carcinoma. *Future Oncol*. 2011;7:1149-1167.

29. Nakanishi K, Sakamoto M, Yamasaki S, Todo S, Hirohashi S. Akt phosphorylation is a risk factor for early disease

recurrence and poor prognosis in hepatocellular carcinoma. *Cancer*. 2005;103:307-312.

30. Viallard C, Larrivée B. Tumor angiogenesis and vascular normalization: alternative therapeutic targets. *Angiogenesis*. 2017;20:409-426.

31. Bačić I, Karlo R, Zadro AŠ, Zadro Z, Skitarelić N, Antabak A. Tumor angiogenesis as an important prognostic factor in advanced non-small cell lung cancer (stage IIIA). *Oncol Lett*. 2018;15:2335-2339. doi:10.3892/ol.2017.7576

32. Okamoto T, Usuda H, Tanaka T, Wada K, Shimaoka M. The functional implications of endothelial gap junctions and cellular mechanics in vascular angiogenesis. *Cancers*. 2019; 11:237.

33. Heath VL, Bicknell R. Anticancer strategies involving the vasculature. *Nat Rev Clin Oncol*. 2009;6:395-404.

34. Wei W, Mok SC, Oliva E, Kim SH, Mohapatra G, Birrer MJ. FGF18 as a prognostic and therapeutic biomarker in ovarian cancer. *J Clin Investig*. 2013;123:4435-4448.

35. Li SH, Tian H, Yue WM, et al. Overexpression of metastasis-associated protein 1 is significantly correlated with tumor angiogenesis and poor survival in patients with early-stage non-small cell lung cancer. *Ann Surg Oncol*. 2011;18: 2048-2056.

36. Trivella M, Pezzella F, Pastorino U, Harris AL, Altman DG. Microvessel density as a prognostic factor in non-small-cell lung carcinoma: a meta-analysis of individual patient data. *Lancet Oncol*. 2007;8:488-499.

37. Sandler A, Gray R, Perry MC, et al. Paclitaxel-carboplatin alone or with bevacizumab for non-small-cell lung cancer. *New Engl J Med*. 2006;355:2542-2550.

38. Nilsson M, Heymach JV. Vascular endothelial growth factor (VEGF) pathway. *J Thorac Oncol*. 2006;1:768-770.

39. Tabernero J. The role of VEGF and EGFR inhibition: implications for combining anti-VEGF and anti-EGFR agents. *Mol Cancer Res*. 2007;5:203-220.

40. Cao W, Zhao Y, Wang L, Huang X. Circ0001429 regulates progression of bladder cancer through binding miR-205-5p and promoting VEGFA expression. *Cancer Biomark*. 2019;25:101-113.

41. Wang Y, Zhang F, Wang J, et al. lncRNA LOC100132354 promotes angiogenesis through VEGFA/VEGFR2 signaling pathway in lung adenocarcinoma. *Cancer Manag Res*. 2018;10:4257-4266.

42. Sadremomtaz A, Mansouri K, Alemzadeh G, Safa M, Rastaghi AE, Asghari SM. Dual blockade of VEGFR1 and VEGFR2 by a novel peptide abrogates VEGF-driven angiogenesis, tumor growth, and metastasis through PI3K/AKT and MAPK/ERK1/2 pathway. *Biochim Biophys Acta Gen Subj*. 2018;1862:2688-2700.

43. Murad W, Rabinowitz I, Lee FC. Sorafenib-induced grade four hepatotoxicity in a patient with recurrent gastrointestinal stromal tumor (GIST): a case report and review of literature. *ACG Case Rep J*. 2014;1:115-117.

44. Multhoff G, Molls M, Radons J. Chronic inflammation in cancer development. *Front Immunol*. 2012;2:98.

45. Hanahan D, Weinberg RA. The hallmarks of cancer. *Cell*. 2000;100:57-70.

46. Xing B, Yang D, Guo W, et al. Ag+ as a more effective elicitor for production of tanshinones than phenolic acids in Salvia miltiorrhiza hairy roots. *Molecules*. 2014;20:309-324.

47. Lei W, Li X, Li L, et al. Compound Danshen Dripping Pill ameliorates post ischemic myocardial inflammation through synergistically regulating MAPK, PI3K/AKT and PPAR signaling pathways. *J Ethnopharmacol*. 2021;281:114438.

48. Tu J, Guo Y, Hong W, et al. The regulatory effects of paeoniflorin and its derivative paeoniflorin-6'-O-benzene sulfonate CP-25 on inflammation and immune diseases. *Front Pharmacol*. 2019;10:57.

49. Gong WG, Lin JL, Niu QX, et al. Paeoniflorin diminishes ConA-induced IL-8 production in primary human hepatic sinusoidal endothelial cells in the involvement of ERK1/2 and akt phosphorylation. *Int J Biochem Cell Biol*. 2015;62: 93-100.

50. Xie T, Li K, Gong X, et al. Paeoniflorin protects against liver ischemia/reperfusion injury in mice via inhibiting HMGB1-TLR4 signaling pathway. *Phytother Res*. 2018;32:2247-2255.

51. Hu S, Sun W, Wei W, et al. Involvement of the prostaglandin E receptor EP2 in paeoniflorin-induced human hepatoma cell apoptosis. *Anticancer Drugs*. 2013;24:140-149.

52. Hu S, Shen G, Zhao W, Wang F, Jiang X, Huang D. Paeonol, the main active principles of Paeonia moutan, ameliorates alcoholic steatohepatitis in mice. *J Ethnopharmacol*. 2010; 128:100-106.

53. Chunhu Z, Suiyu H, Meiqun C, Guilin X, Yunhui L. Antiproliferative and apoptotic effects of paeonol on human hepatocellular carcinoma cells. *Anticancer Drugs*. 2008; 19:401-409.

54. Ding Y, Li Q, Xu Y, et al. Attenuating oxidative stress by paeonol protected against acetaminophen-induced hepatotoxicity in mice. *PLoS One*. 2016;11(5):e0154375.

55. Cheng GY, Jiang Q, Deng AP, et al. CD31 induces inflammatory response by promoting hepatic inflammatory response and cell apoptosis. *Eur Rev Med Pharmacol Sci*. 2018;22:7543-7550.

56. Fornasa G, Groyer E, Clement M, et al. TCR stimulation drives cleavage and shedding of the ITIM receptor CD31. *J Immunol*. 2010;184:5485-5492.

57. Peng KY, Gu JF, Su SL, et al. Salvia miltiorrhiza stems and leaves total phenolic acids combination with tanshinone protect against DSS-induced ulcerative colitis through inhibiting TLR4/PI3K/AKT/mTOR signaling pathway in mice. *J Ethnopharmacol*. 2021;264:113052.